Looking for z>7 galaxies with the Gravitational Telescope

R. Pelló[1], J. Richard[1], D. Schaerer[2,1], J. F. Le Borgne[1], J. P. Kneib[3], A. Hempel[2]
(1) Observatoire Midi-Pyrénées, Laboratoire d'Astrophysique, UMR 5572, 14 Avenue E. Belin, F-31400 Toulouse, France
(2) Geneva Observatory, 51 Ch. des Maillettes, CH–1290 Sauverny, Switzerland
(3) OAMP, Laboratoire d'Astrophysique de Marseille, UMR 6110 traverse du Siphon, 13012 Marseille, France

Abstract. We summarize the main results obtained recently by our group on the identification and study of very high-z galaxies (z>7) using lensing clusters as natural gravitational telescopes. A description of our pilot survey with ISAAC/VLT is presented, aimed at the spectroscopic confirmation of z>7 candidate galaxies photometrically selected from deep near-IR, HST and optical ground-based imaging. The first results issued from this survey are discussed, in particular the global photometric properties of our high-z candidates, and the implications for the global star formation rate at very high-z.

1 Introduction

Considerable advances have been made during the last decade in the exploration of the early Universe, from the discovery and detailed studies of redshift $z \sim 3$ galaxies (the so-called Lyman break galaxies, LBGs, e.g. Steidel et al. 2003), over $z \sim 4$–5 galaxies found from numerous deep multi-wavelength surveys, to galaxies at $z \sim 6$–7, close to the end of reionisation epoch of the Universe (e.g. Hu et al. 2002, Kodaira et al. 2003, Cuby et al. 2003, Kneib et al. 2004, Stanway et al. 2004, Bouwens et al. 2004b). Extending the searches beyond $z \simeq 6.5$ and back to ages where the Universe was being re-ionized (cf. Fan et al. 2002) requires extremely deep observations in the near-IR bands. Indeed, astounding depths can be reached in ultra-deep fields, such as demonstrated e.g. recently with J and H imaging of the NICMOS Ultra-Deep Field (UDF; Thompson et al. 2005; Bouwens et al. 2004a, Bouwens et al. 2005) from which 5 faint ($H_{AB} \sim 27$) candidates at $z \sim 7$–8 have been identified (Bouwens et al. 2004b).

We present in this paper a summary of our results on a deep survey of lensing clusters with ISAAC/VLT, aimed at constraining the abundance of star-forming galaxies at $z \sim 6-11$ taking benefit from lensing magnification to improve the search efficiency and subsequent spectroscopic studies (see more details in Pello et al. 04 and Richard et al. 05). We briefly describe the photometric technique used to identify very high-z objects, the construction and analysis of the photometric catalogs, the luminosity funtions (LFs) derived for star-forming galaxies up to $z \sim 10$, and the implications for the cosmic SFR. Throughout this paper we adopt standard cosmological parameters ($\Omega_\Lambda = 0.7$, $\Omega_m = 0.3$, $H_0 = 70\ km\ s^{-1}\ Mpc^{-1}$).

2 Photometric Survey and Selection of High-z Candidates

The objective of our Survey was to obtain deep near-IR photometry from 1.0 to 2.4 μm, in order to derive accurate photometric redshifts for optical dropouts in the critical domain $6 \leq z \leq 11$. Simulations have been done to define the observing strategy to target high-z sources using the evolutionary synthesis models by Schaerer (2002, 2003) for Population III and extremely metal deficient starbursts, together with the usual templates for normal galaxies. The main relevant signatures of genuine star-forming sources at $z > 7$, which are common to all models, are well known: they are optical dropouts, displaying a strong break and "red" optical vs. IR colors, whereas they exhibit a "blue" SED redwards due to UV rest-frame emission. Different redshift intervals are defined using the appropriate set of near-IR filters in combination with optical data through the Lyman break technique, by constraining both the position of the break and the restframe UV slope. Figure 1 illustrates this technique in the $8 \leq z \leq 11$ domain.

The two lensing clusters used in this study were AC114 ($z = 0.312$) and Abell 1835 ($z = 0.252$). AC114 is a well-known gravitational telescope, with a lens model well-constrained by a large number of multiple-images at high-z (Smail et al. 1995, Natarajan et al. 1998, Campusano et al. 2001). A1835 is the most X-ray luminous cluster in the $XBACS$ sample (Ebeling et al. 1998), thus potentially one of the most efficient gravitational telescopes. We observed these clusters in the ~ 0.9 to 2.2 μm domain between September 2002 and April 2004, covering as far as possible the z, SZ, J, H, and K bands. Optical images between U and I bands were available from previous surveys and data archives (Table 1).

Near infrared photometry of extremely faint sources requires a careful data reduction, described in details by Richard et al. (2005). In summary, after a standard pre-reduction (ghost, dark and flat-field corrections),

Table 1: Summary of the photometric dataset used in this Survey: filter, exposure time, seeing (original images), pixel size, 1 σ limiting magnitude within 1.5 $''$ diameter aperture, filter effective wavelength, AB correction ($m_{AB} = m_{Vega} + C_{AB}$), and references (see Richard et al. 2005 for details).

	Filter	t_{exp} [ksec]	seeing [$''$]	pix [$''$]	depth [mag]	λ_{eff} [nm]	C_{AB} [mag]	Reference
AC114	U	20.00	1.3	0.36	29.1	365	0.693	Barger et al. 1996
	B	9.00	1.2	0.39	29.0	443	-0.064	Couch et al. 2001
	V	21.60	1.1	0.47	28.5	547	0.022	Smail et al. 1991
	R^2_{702}	$\geq$ 24.90	0.13	0.100	$\geq$ 28.4	700	0.299	Natarajan et al. 1998
	I_{814}	20.70	0.3	0.100	26.8	801	0.439	Smail et al. 1991
	J	6.48	0.52	0.148	25.5	1259	0.945	Richard et al. 05
	H	13.86	0.40	0.148	24.7	1656	1.412	Richard et al. 05
	Ks	18.99	0.34	0.148	24.3	2167	1.873	Richard et al. 05
A1835	V	3.75	0.76	0.206	28.1	543	0.018	Czoske et al. 2002
	R	5.40	0.69	0.206	27.8	664	0.246	Czoske et al. 2002
	R_{702}	7.50	0.12	0.100	27.7	700	0.299	Smith et al. 2003
	I	4.50	0.78	0.206	26.7	817	0.462	Czoske et al. 2002
	z	6.36	0.70	0.252	26.7	919	0.554	Richard et al. 05
	SZ	21.96	0.54	0.148	26.9	1063	0.691	Richard et al. 05
	J	6.48	0.65	0.148	25.6	1259	0.945	Richard et al. 05
	H	13.86	0.50	0.148	24.7	1656	1.412	Richard et al. 05
	Ks	18.99	0.38	0.148	24.7	2167	1.873	Richard et al. 05

we used the IRAF package XDIMSUM[1] for a two-step sky-subtraction. During the first pass, each image is sky-subtracted using the sky pattern obtained from a group of adjacent frames and a bad-pixel mask is created in the process. Images are registered and combined using integer shifts values to preserve the noise properties, with bad-pixel rejection. Then, sources are detected in order to create an object mask, and a second sky-subtraction is applied to the data. Several versions of the final images were produced, using slightly different reduction recipes, in order to cross-check the final catalogs.

Photometry in the near-IR bands was obtained after matching all images to a common seeing with a gaussian convolution, the worst case being the J band for both clusters. The *SExtractor* package (Bertin & Arnouts 1996) was used for source detection and photometry. We optimized the parameters to detect very faint unresolved sources, in order to build an H-band selected sample. The original images were used to derive the error bars in each band through detailed simulations. Also limiting magnitudes in the Table 1 and completeness levels in the different filters were obtained in this way. The final catalogs include photometry within 1.5$''$ apertures for all objects detected in the H band; we were able to measure photometry of very faint sources ($J \sim 24.4 - 24.8$, H and $Ks \sim 23.5$) with a relatively good accuracy (S/N$\geq$ 3-4). The fraction of spurious detections expected in our photometric catalogs, for objects detected *only* in the reference filter H, was estimated from a special H band *noise image* where all astronomical sources were removed by subtracting by pairs sequential images acquired with similar seeing conditions, and then coadding them using the same procedure as for astronomical images. The result is an image with the same noise properties compared to the final stacks, but without astronomical sources. We find that for the faintest magnitude bins considered in this survey, the *maximum number of false-positive detections* should be typically lower than 50 %, for sources detected *only* in the reference filter H, and no spurious detections are expected up to $H = 23.0$ (AB$\sim$ 24.4).

A catalog of optical dropouts was selected (i.e., objects non-detected in all the optical images, from U to z bands). First-category sources are those detected in at least two near-IR bands. Among them, $\sim$ 89% of sources detected in the H-band reference image in A1835 (and 75% in AC114) are also re-detected in the pseudo-χ^2 image. The later was obtained from the combination of individual J, H and Ks images, normalized by the noise 1σ image, and weighted by the square root of the corresponding exposure-time maps. After careful manual inspection, the final catalog of first/second-category dropouts for Abell 1835 and AC114 contains 18/6 and 8/2 sources respectively, and number of third category sources (dubious after manual inspection, detected only in the reference filter) close to the critical lines.

The position of optical dropouts in the different color-color diagrams provides an estimate of their photometric redshift, and an objective criterium to classify them into different z intervals. The majority of optical dropouts in the two clusters fulfill the high-z requirements in Fig. 1. Those located in the $0 \leq z \leq 8$ region of the diagram fulfill the ERO selection criterium ($R - K > 5.6$), and some of them could be intermediate-redshift dusty starbursts. The $SZJH$ and $zSZJ$ color-color diagrams were used to select candidates in the range $7 \leq z \leq 8.5$ and $6 \leq z \leq 7.5$ respectively. For about 30% of our candidates, the S/N is enough to derive photometric redshifts based on SED-fitting using an adapted version of the public software $Hyperz$ (Bolzonella et al. 2000). Objects unambiguously identified as low-z galaxiess are excluded from the sample, as well as sources whose nature could not be determined with the present data (either variable sources or "bright" EROs with ambiguous but plausible low-z solutions).

[1]XDIMSUM is a modified version by the IRAF group of the Deep Infrared Mosaicing Software package by P. Eisenhardt et al. See ftp://iraf.noao.edu/extern-v212/xdimsum for details

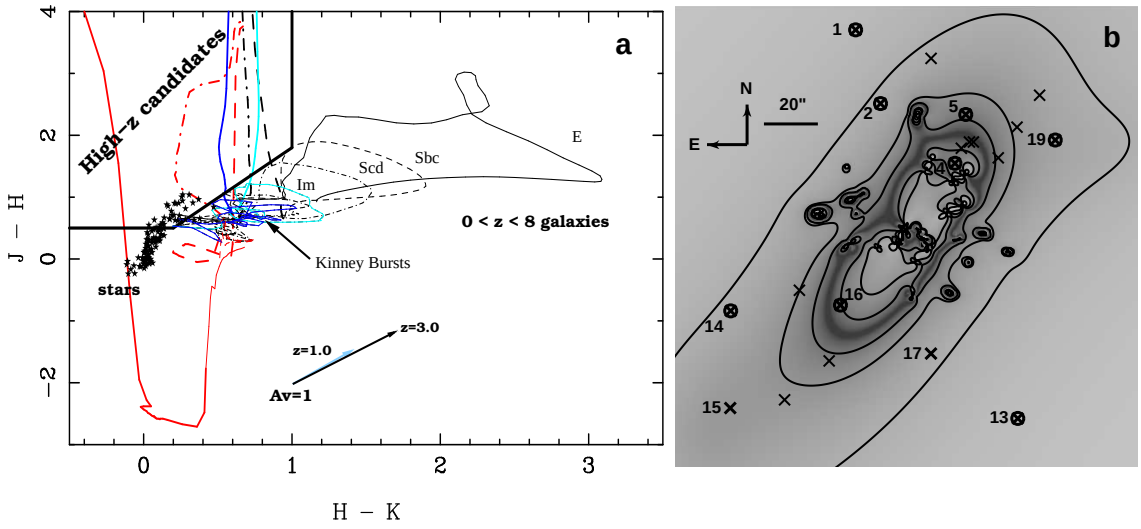

Figure 1: **a:** $J-H$ versus $H-Ks$ color-color diagram (Vega system) showing the position expected for different objects over the interval $z \sim 0$ to 11. The position of stars and normal galaxies up to $z \leq 8$ are shown, as well as the shift direction induced by $A_V = 1$ magnitude extinction. Thin and thick lines display models below and above $z = 8$ respectively. Several models for Pop III starbursts are presented, for different fractions of Lyman-α emission flux entering the integration aperture: 100% (red solid line), 50% (red dashed line) and 0% (red dot-dashed line). The location of Kinney et al. (1996) starbursts templates is also given for comparison (SB1(cyan) and SB2 (blue)). All star-forming models enter the high-z candidate region at $z \geq 8$. **b:** Location of first and second category photometric candidates in the lensing cluster AC114 (circles and crosses respectively). Contours are overplotted for magnification values of 1, 2 and 3 magnitudes, computed assuming sources at $z = 9$, although the position of these lines is weakly sensitive to source redshift within the relevant $z \sim 6-10$.

High-z candidates were selected based *only* on their photometric properties, irrespective of their positions with respect to the critical lines. However, objects located close to the high-z critical lines are of greater interest, because of the larger magnification. The *minimum* magnification factor over the region covered by our near-IR survey is at least ~ 0.7 magnitudes, and at least ~ 1 magnitude over 50 % of the ISAAC field of view. Thus, the *effective* 3σ limiting magnitudes reached here are, at worst, similar to those attained in the HDFS (Labbé et al. 2003) in $JHKs$ (respectively AB$\sim$ 26.8, 26.2 and 26.2). Our 3σ limiting magnitudes in the H band are also very close to the typical magnitudes of the $z \sim 7-8$ z-dropouts detected by Bouwens et al. (2004b) in the Hubble Ultra Deep Field, with $H_{160}(AB) \sim 26.0$ to 27.3, after correction for a typical magnification factor of at least ~ 1 magnitude.

3 Luminosity Function and Cosmic Star Formation Rate

The typical magnification values of our candidates range between 1.5 (~ 0.44 mags) and 10 (2.5 mags). For some objects very close to the critical lines, we found magnifications values $\mu > 25$. Interestingly, although the selection criteria are only based on near-IR colors irrespective of magnitudes, *almost all* the photometric candidates fulfilling our selection criteria turn out to be *fainter* than $H = 23.0$ (AB $\sim$ 24.5). Only three exceptions are found in Abell 1835 among the possible low-z EROs, as described above. After correction for magnification accross these fields, the lack of "bright" sources means that we have not detected young starbursts at $z \sim 6-10$ more massive than typically a few 10^8 $M_\odot$ (under standard assumptions for the IMF).

We derived the unlensed L_{1500} luminosity, at 1500 Å restframe, for all high-z candidates, using the adopted photometric redshift. L_{1500} luminosities were converted into Star Formation Rate (SFR) through the usual calibration from Kennicut (1998). The typical SFR obtained for objects included in the final sample is ~ 10 $M_\odot$ yr^{-1}, with extreme values ranging from a few units to ~ 20 $M_\odot$ yr^{-1}. The restframe UV slope of our candidates is extremely blue, usually ranging between -1.5 and -3.5, a systematic trend also reported by Bouwens et al. (2004b) for their sample of $z \sim 7-8$ candidates. Although optical-dropouts are stretched by the magnification factor μ, they appear as point-like sources in our ground-based images. The physical size of these objects at $z > 7$ is likely to be smaller than 1.7 kpc, with the magnification factors involved.

Magnification and dilution effects by the lensing field were carefully taken into account to compute number densities and derived quantities, in particular to estimate the LF at 1500 Å . The observed sample of candidates was also corrected for incompleteness using mock simulations (see details in Richard et al. 2005). The combined L_{1500} LFs for both clusters, with the corresponding error-bars, are given in Fig. 2. Only first-priority candidates

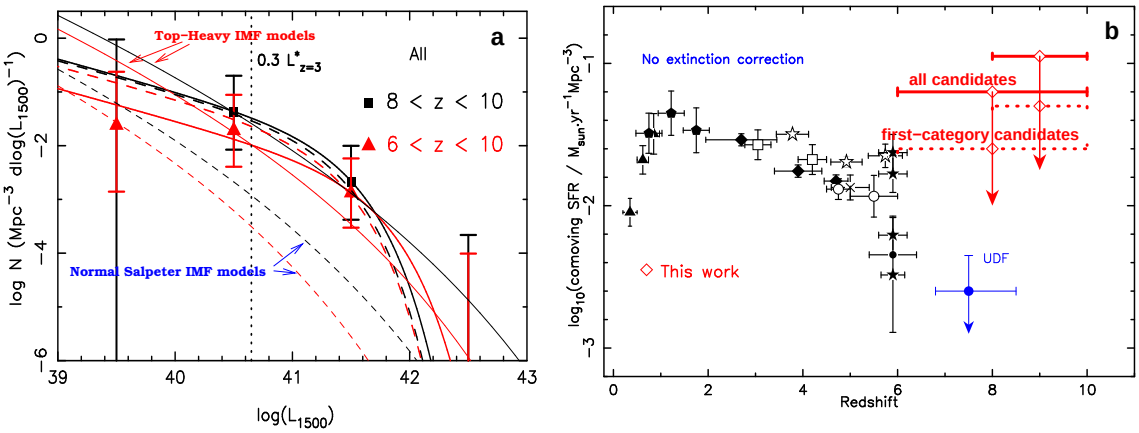

Figure 2: **a:** L_{1500} LFs derived for the photometric sample of high-z candidates in this survey (adapted from Richard et al. 05). z intervals shown are: $z = 6-10$ (red) and $z = 8-10$ (black). Errors include Poisson noise statistics and lensing uncertainties. STY fits to the LF data are presented by thick solid lines, and compared to the LF by Steidel et al. for LBGs at $z \sim 4$ (thick dashed line), with the usual $(1+z)^{-1}$ correction, *without any additional renormalization*. We also display the LFs corresponding to simple models, for 2 extreme IMF assumptions discussed in the text. **b:** Evolution of the comoving SFR density as a function of redshift. Our upper limits are compared to other surveys, uncorrected for extinction (adapted from Bunker et al. 2004, and references herein): data compiled from the CFRS (Lilly et al. 1996, filled triangles), Connolly et al. 1997 (filled pentagons), LBG work from Steidel et al. 1999 (open squares), Fontana et al. 2003 (open circles), Iwata et al. 2003 (cross), Bouwens et al. 2003a (filled diamonds), GOODS (Giavalisco et al. 2004, open stars), ACS estimates by Bouwens et al. 2003b (filled stars) and Bunker et al. 2004 (filled circle). The value derived by Bouwens et al. (2004b) in the UDF is also shown. Our results are displayed for all (solid) and first-category (dashed) candidates.

have been considered, but the difference obtained when using the full sample is within 1σ error bars. STY fits (Sandage, Tammann & Yahil 1979) to the data are also presented in Fig. 2. The typical value found for L^* is $10^{41.5}$ ergs s^{-1} s^{-1} Å $^{-1}$, with a fixed value $\alpha = 1.6$ (i.e., Steidel et al. (1999) determination for LBGs at $z \sim 4$). The STY fit to the data is in remarkably good agreement with the LF found by Steidel et al. for LBGs at $z \sim 4$, with the usual $(1+z)^{-1}$ correction to account for the surface brightness increase with redshift due to size scaling for a fixed luminosity, *without any additional renormalization*. A fairly good agreement is also found when comparing with the LF derived by Bunker et al. (2004) for their sample of $z \sim 6$ candidates in the UDF, i.e. a density of sources $\sim 1/6$ (-0.8 dex) smaller as compared to LBGs at $z \sim 4$, still within our 1σ error bars. We compare the observed LFs to the predictions obtained from a simple model for halo formation based on Press-Schechter formalism, assuming that all haloes convert a constant fraction ~ 0.1 of their baryonic mass into stars somewhen between $z = 17$ and $z = 6$, with a correction for the visibility time of starbursts, and using two extreme IMF assumptions: a standard Salpeter and a top-heavy IMF (stars between 50 and 500 $M_\odot$). "Top heavy" IMF models provide a better fit for the bright end of the LF, but this simple model can hardly explain simultaneously the behaviour of the bright and faint ends of the LF.

Figure2 displays the upper limits for the Cosmic SFR value obtained for each redshift bin, by integrating the LFs down to 0.3 $L^*_{z=3}$, compared to other surveys.

4 Discussion and Conclusions

Taken at face value, the cosmic SFR density found in this survey is in good agreement with the theoretical estimates for the redshift domain considered here derived by Barkana & Loeb (2001; see their Fig. 29), for a reionization redshift $\sim 8-6$. However, there is a discrepancy by a factor of ~ 10 between our results and previous studies at similar redshifts, in particular in the UDF (Bouwens et al. 2004, 2005). In all cases, the sources detected are photometric candidates, and thus upper limits to the actual UV flux densities. The effective fields surveyed are dramatically small, thus leading to strong field-to-field variations in the number of sources. Cluster-to-cluster fluctuations are clearly seen in our sample, although lensing and photometric considerations could account for most of them. A positive magnification bias could still be present in this survey (the incompleteness of our sample in the relevant magnitude domain is smaller than in blank-field surveys), producing a systematic trend as compared to blank fields. Could this result be confirmed on a larger sample of lensing clusters and

blank fields, the slope of the number counts at $z \sim 6-10$ could be precisely constrained, at least for the brightest part of the LF.

Up to now, our spectroscopic survey with ISAAC has targeted 2 candidates in AC114, and 7 in Abell 1835 (4 first priority targets and 3 secondary ones; Pelló et al. 2004); 2/3 of objects in this sample display emission lines. The efficiency of our survey nowadays could range between ~ 30 and 50%, with interesting low-z by-products. A large majority of our high-z candidates still need to be confirmed, either by a redetection of the faint emission line, or by the non-detection of other lines expected at low-z.

The results presented here are to be confirmed in different ways. An enlarged spectroscopic survey is urgently needed to determine the efficiency of our selection technique. Also, increasing the number of lensing fields with ultra-deep near-IR photometry is essential to get tighter constraints on the abundance and physical properties of $z \geq 7$ starburst galaxies.

Acknowledgements. Based on observations collected at the European Southern Observatory, Chile (069.A-0508,070.A-0355,073.A-0471), the NASA/ESA Hubble Space Telescope operated by the Association of Universities for Research in Astronomy, Inc., and the Canada-France-Hawaii Telescope operated by the National Research Council of Canada, the French Centre National de la Recherche Scientifique (CNRS) and the University of Hawaii. Part of this work was supported by the CNRS and the Swiss National Foundation.

References

[1] Barkana, R. & Loeb, A. , 2001, Physics Reports, 349, 125

[2] Bertin, E., Arnouts, S., 1996, A & AS, 117,393.

[3] Bolzonella, M., Miralles, J.M., Pelló, R., 2000, A & A, 363, 476.

[4] Bouwens, R. J., Illingworth, G. D., Blakeslee, J. P., Broadhurst, T. J., & Franx, M. 2004a, ApJ 611, L1.

[5] Bouwens R. J., Thompson R. I., Illingworth G. D., et al. 2004b, ApJ 616, L79

[6] Bouwens, R. J., Illingworth, G. D., Thompson, R. I., Franx, M., 2005, ApJ, 624, L5.

[7] Bunker, A. J., Stanway, E. R., Ellis, R. S., & McMahon, R. G. 2004, MNRAS, 355, 374

[8] Campusano, L.E., Pelló, R., Kneib, J.-P., et al. 2001, A & A, 378, 394.

[9] Cuby, et al. 2003, A&A 405, L19.

[10] Ebeling, H., Edge, A. C., Bohringer, H., et al. 1998, MNRAS, 281, 799.

[11] Fan, X., et al. 2002, AJ, 123, 1247.

[12] Giavalisco M., et al., 2004, ApJ, 600, L103.

[13] Hu, E. M., Cowie, L. L., McMahon, R. G., et al. 2002, ApJ 568, L75.

[14] Kennicutt, R. C. 1998, ARA&A, 36, 189

[15] Kneib, J.-P., Ellis, R.S., Santos, M.R., Richard, J., 2004, ApJ 607, 697.

[16] Kodaira, K., et al. 2003, PASPJ 55, L17.

[17] Labbé, I., Franx, M., Rudnick, G., et al. 2003, AJ, 125, 1107.

[18] Lilly, S. J., Le Fevre, O., Hammer, F., & Crampton, D. 1996, ApJ 460, L1.

[19] Natarajan, P., Kneib, J.-P., Smail, I., Ellis, R.S., 1998, ApJ, 499, 600.

[20] Pelló, R., Schaerer, D., Richard, J., Le Borgne, J.-F., Kneib, J.-P., 2004, IAU Symp. No. 225: The Impact of Gravitational Lensing on Cosmology, Y. Mellier and G. Meylan, Eds., [astro-ph/0410132]

[21] Richard, J., Pello, R., Schaerer, D., Le Borgne, J. F., Kneib, J.-P., 2005, submitted to A & A

[22] Sandage, A., Tammann, G. A. & Yahil, A. 1979, ApJ 232, 352

[23] Schaerer, D. 2002, A & A 382, 28.

[24] Schaerer, D. 2003, A & A 397, 527.

[25] Smail, I., Couch, W.J., Ellis, R.S., Sharples, R.M., 1995, ApJ, 440, 501.

[26] Stanway, E. R., Bunker, A. J., McMahon, R. G., et al. 2004, ApJ, 607, 704

[27] Steidel, C. et al., 2003, ApJ 592, 728.

[28] Thompson, R.I., Illingworth, G., Bouwens, R., et al., 2005, AJ, 130, 1.